Journal of Nuclear Materials 385 (2009) 419–423

Contents lists available at ScienceDirect

Journal of Nuclear Materials

journal homepage: www.elsevier.com/locate/jnucmat

Oxygen potentials of mixed oxide fuels for fast reactors

M. Kato [a,*], T. Tamura [b], K. Konashi [c]

[a] Nuclear Fuel Cycle Engineering Laboratories, Japan Atomic Energy Agency, 4-33, Tokai-mura, Naka-gun, Ibaraki 319-1194, Japan
[b] Inspection Development Company, 4-33, Tokai-mura, Naka-gun, Ibaraki 319-1194, Japan
[c] Tohoku University, 2145-2, Narita, Oarai-machi, Ibaraki 311-1313, Japan

ARTICLE INFO

PACS:
28.41.Bm
28.50.Ft
65.40.-b

ABSTRACT

Oxygen potentials of homogenous $(Pu_{0.2}U_{0.8})O_{2-x}$ and $(Am_{0.02}Pu_{0.30}Np_{0.02}U_{0.66})O_{2-x}$ which have been developed as fuels for fast breeder reactors were measured at temperatures of 1473–1623 K by a gas equilibrium method using an (Ar, H_2, H_2O) gas mixture. The measured oxygen potentials of $(Pu_{0.2}U_{0.8})O_{2-x}$ were about 25 kJ mol^{-1} lower than those of $(Pu_{0.3}U_{0.7})O_{2-x}$ measured previously and were consistent with the values calculated by Besmann and Lindemer's model. The measured oxygen potentials of $(Am_{0.02}Pu_{0.30}Np_{0.02}U_{0.66})O_{2-x}$ were slightly higher than those of MOX without minor actinides. No fuel-cladding chemical interaction is affected significantly by adding their minor actinides.

1. Introduction

Plutonium and uranium mixed oxide (MOX) fuels with Pu fractions of about 20% and 30% have been produced, respectively, as fuels for the inner and outer core in the fast reactor 'Monju' [1]. Furthermore, homogenous MOX fuels containing minor actinide (MA) elements such as Np and Am have also been produced by the Japan Atomic Energy Agency (JAEA) in the frame of an advanced nuclear recycle program [2–6]. The MOX fuels are oxygen nonstoichiometric compounds and are stable in a wide range of both hyper- and hypo-stoichimetric compositions [6–8]. Physical properties of the oxides such as thermal conductivities and melting temperatures depend significantly on oxygen-to-metal (O/M) molar ratio [6,9–11].

A dependency of the O/M molar ratio on an oxygen potential ($\Delta\bar{G}_{O_2}$) of the MOX fuel is also important for evaluating the chemical behavior on the fuel pin. Fuel-cladding chemical interaction (FCCI) occurs on the inner surface of cladding at high burn-up and it limits the operating time. Since the O/M molar ratio increases with increasing fuel burn-up, the corrosion environment in a fuel pin with high burn-up becomes more severe than that at the beginning of irradiation. Therefore, the as-fabricated O/M ratio is one of the important parameters for controlling FCCI and determining fuel lifetime. Low O/M mixed oxide fuel has been developed to attain high burn-up of more than 100 GW d t^{-1} [12].

There are many studies about $\Delta\bar{G}_{O_2}$ of the MOX fuel in relation to its Pu content, O/M molar ratio and temperature [13–23]. It was reported that the $\Delta\bar{G}_{O_2}$ increases with Pu fraction y of the $(Pu_yU_{1-y})O_{2-x}$ fuel [24–26]. However, experimental data were scattered over ranges of more than ±100 kJ mol^{-1}, and it was difficult to understand the dependency of $\Delta\bar{G}_{O_2}$ on Pu content, especially in the near stoichiometric composition i.e. with $0.02 < x < 0.00$. The present authors have also measured $\Delta\bar{G}_{O_2}$ for $(Pu_{0.3}U_{0.7})O_{2-x}$ by thermogravimetry in a previous report [13]. In this work, $\Delta\bar{G}_{O_2}$ of $(Pu_{0.2}U_{0.8})O_{2-x}$ (with $x = 0.0090$–0.0000) and $(Am_{0.02}Pu_{0.30}Np_{0.02}U_{0.66})O_{2-x}$ (with $x = 0.0129$–0.0000) were accurately measured by a thermogravimetric technique to obtain basic data for the irradiation behavior evaluation.

2. Experimental

2.1. Sample preparation

The plutonium-to-uranium ratio was controlled in the nitrate solution of $(Pu_{0.2}U_{0.8})O_2$ starting material. The $(Pu_{0.2}U_{0.8})O_2$ powder was prepared by the denitration method using microwave direct heating. The $(Pu_{0.2}U_{0.8})O_2$ powder was then pressed and sintered at 1973 K for 3 h in (Ar, 5% H_2)mixed gas to make pellets (5.4 mm diameter). Another sample of $(Am_{0.02}Pu_{0.30}Np_{0.02}U_{0.66})O_{2-x}$ was prepared by a mechanical blending process from $(Pu_{0.30}Np_{0.06}U_{0.64})O_2$, $(Am_{0.07}Pu_{0.93})O_2$ and UO_2 powders. After mixing the powders for 4 h with a ball mill, pellets of $(Am_{0.02}Pu_{0.30}Np_{0.02}U_{0.66})O_2$ were prepared by pressing and sintering at 1973 K for 3 h in (Ar, 5% H_2) mixed gas with added moisture. Chemical analysis showed that the total of metallic impurities was less than 500 ppm. The homogeneity of sample was confirmed by an X-ray diffractometry (XRD) and investigations with electron probe micro analyzer (EPMA).

* Corresponding author. Tel.: +81 29 282 1111; fax: +81 29 282 9473.
E-mail address: kato.masato@jaea.go.jp (M. Kato).

0022-3115/$ - see front matter © 2008 Elsevier B.V. All rights reserved.
doi:10.1016/j.jnucmat.2008.12.012

2.2. Measurement procedure

Sintered pellets were crushed in an agate mortar and then annealed to adjust the O/M functions to the stoichiometric composition at 1123 K for 8 h in an atmosphere of $\Delta\bar{G}_{O_2} = -420 \pm 1$ kJ mol^{-1}. The weights of samples for the measurement of $\Delta\bar{G}_{O_2}$ were 140–200 mg. The measurements were carried out by the thermal gravimetry and differential thermal analysis (TG-DTA) method. The TG-DTA apparatus (Rigaku TG8120 model) was installed in a glove box isolated from vibration by air dampers. The O/M molar ratio changes were driven by the oxygen partial pressure (P_{O_2}) itself was controlled by the H_2/H_2O ratio in the annealing atmosphere. The x value was calculated from the weight change of the sample using the following relationship:

$$x = 16.894 \cdot (\Delta W/W), \tag{1}$$

where ΔW is the change of sample weight and W is the sample weight for a O/M molar ratio of 2.0000. A horizontal differential type balance was used and it could measure weight changes of ±1 μg that corresponded to O/M molar ratio changes of ±0.00015.

The $\Delta\bar{G}_{O_2}$ of the device atmosphere was controlled by the H_2O/H_2 ratio. Considering the reaction of $H_2O \leftrightarrow H_2 + 1/2O_2$, the equilibrium of the H_2O/H_2 system may be expressed by a formation free energy given by:

$$\Delta G_f = -RT \ln \frac{p^*_{H_2O}}{(p^*_{H_2} \cdot p^*_{O_2})^{1/2}} \tag{2}$$

Where R in gas constant (8.3145 J mol^{-1} K^{-1}), T is the absolute temperature (K) and p^*_i is partial pressure of phase i, which is derived from the ratio of partial pressure to its standard state, 0.101 MPa. The Standard Gibbs free energy of formation, ΔG_f, can be calculated using the following equation:

$$\Delta G_f = -246440 + 54.81 \cdot T. \tag{3}$$

The $p^*_{O_2}$ was measured at 973 K using stabilized zirconia oxygen sensor. The $p^*_{H_2O}/p^*_{H_2}$ ratio at 973 K was calculated by Eq. (2). The $p^*_{O_2}$ at the position of the sample was calculated under the assumption that the above ratio of p_{*H_2O}/p_{*H_2} was the same at any sample position. The oxygen potential measurement method used in this work was reported in detail previously [13].

3. Results and discussion

3.1. Oxygen potentials of $(Pu_{0.2}U_{0.8})O_{2-x}$

Equilibrium $p^*_{O_2}$ values were measured at 1473, 1523, 1573 and 1623 K by the gas equilibrium technique. $\Delta\bar{G}_{O_2}$ values were calculated from $p^*_{O_2}$ and temperature using the following equation,

$$\Delta\bar{G}_{O_2} = RT \ln p^*_{O_2}. \tag{4}$$

The measured data of $\Delta\bar{G}_{O_2}$ of $(Pu_{0.2}U_{0.8})O_{2-x}$ are shown as a function of the O/M molar ratio with little scattering in Fig. 1. Fig. 2 plots $\Delta\bar{G}_{O_2}$ together with literature data [16,19,23] for comparison. The present data are consistent with the data reported by Javed [19], but the other literature data [16,23] are 50–100 kJ mol^{-1} higher than those.

$\Delta\bar{G}_{O_2}$ is given by,

$$\Delta\bar{G}_{O_2} = \Delta\bar{H}_{O_2} - T \cdot \Delta\bar{S}_{O_2} \tag{5}$$

where $\Delta\bar{H}_{O_2}$ is partial molecular enthalpy of O_2 and $\Delta\bar{S}_{O_2}$ is partial molecular entropy of O_2 both at T (K). The relation between $\Delta\bar{G}_{O_2}$ of $(Pu_{0.2}U_{0.8})O_{1.995}$ and T is shown in Fig. 3. Literature data [13–15] of $(Pu_{0.3}U_{0.7})O_{1.995}$ are also plotted. The three data sets for $(Pu_{0.3}U_{0.7})O_{1.995}$ are consistent, and $\Delta\bar{H}_{O_2}$ and $\Delta\bar{S}_{O_2}$ are estimated to be −922 kJ mol^{-1} and −300 J mol^{-1} K^{-1}, respectively. However, the data for $(Pu_{0.2}U_{0.8})O_{1.995}$ are scattered. The two broken lines shown in Fig. 3 are values of $(Pu_{0.1}U_{0.9})O_{1.995}$ and $(Pu_{0.4}U_{0.6})O_{1.995}$ which were calculated using the model reported by Besmann and Lindemer [26]. The data of $(Pu_{0.2}U_{0.8})O_{1.995}$ reported by Sørensen [23] and Chilton and Edwards [16] fall on the calculated line of $(Pu_{0.4}U_{0.6})O_{1.995}$. On the other hand, the present data are about 25 kJ mol^{-1} lower than those of $(Pu_{0.3}U_{0.7})O_{1.995}$ and are consistent with the values calculated using the model reported by Besmann and Lindemer [26]. It is considered that Fig. 3 demonstrates the validity of the present data, and oxygen potentials of MOX increase with Pu content.

Substituting Eq. (4) into Eq. (5), the following relationship is obtained.

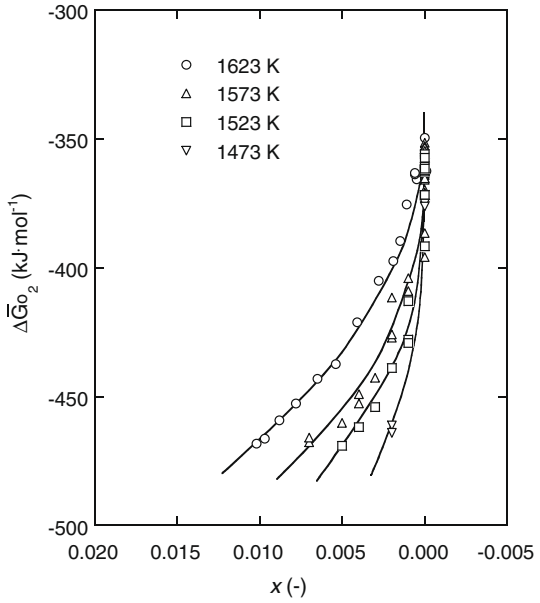

Fig. 1. Oxygen potentials of $(Pu_{0.2}U_{0.8})O_{2-x}$ at temperatures from 1473 to 1623 K.

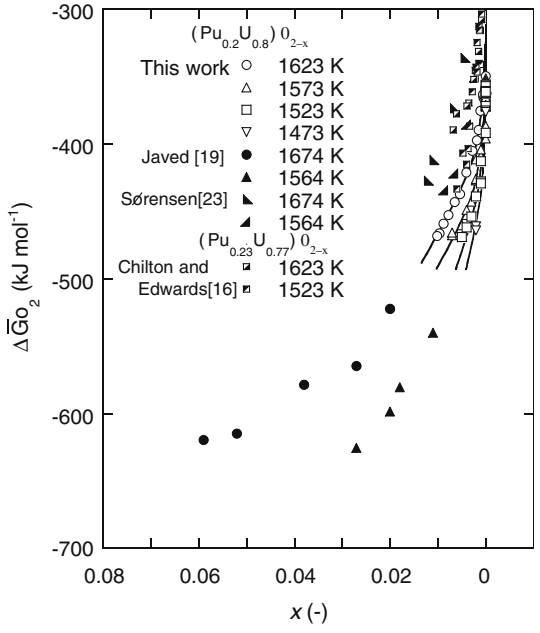

Fig. 2. Oxygen potentials of $(Pu_{0.2}U_{0.8})O_{2-x}$.

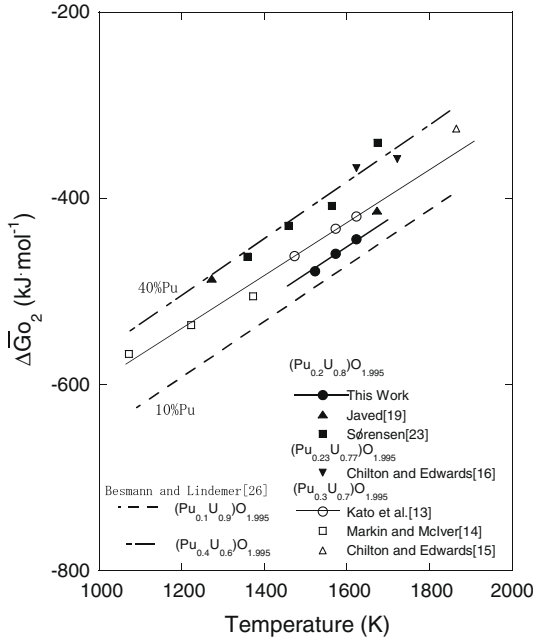

Fig. 3. Oxygen potentials of (Pu, U)$O_{1.995}$ as functions of temperature and Pu content.

$$\ln p^*_{O_2} = \frac{\Delta\bar{H}_{O_2}}{RT} - \frac{\Delta\bar{S}_{O_2}}{R}. \quad (6)$$

The relation between $\ln p^*_{O_2}$ and $1/T$ is shown in Fig. 4. A $\Delta\bar{H}_{O_2}$ value was obtained from the slope in Fig. 4 using Eq. (6). The values of $\Delta\bar{H}_{O_2}$ are −1083, −1038 and −994 kJ mol^{-1} for $(Pu_{0.2}U_{0.8})O_{1.995}$, $(Pu_{0.2}U_{0.8})O_{1.997}$ and $(Pu_{0.2}U_{0.8})O_{1.999}$, respectively. These values are 161–244 kJ mol^{-1} lower than those of $(Pu_{0.3}U_{0.7})O_{2-x}$ as shown in Table 1.

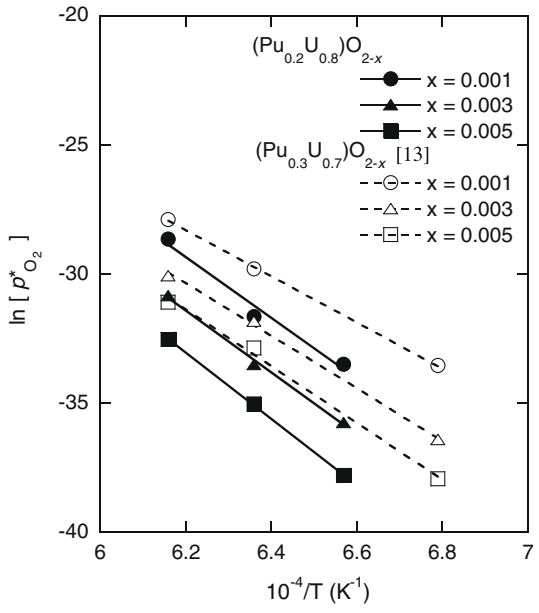

Fig. 4. Relation between $\ln p^*_{O_2}$ and $1/T$ in $(Pu_{0.2}U_{0.8})O_{2-x}$ and $(Pu_{0.3}U_{0.7})O_{2-x}$.

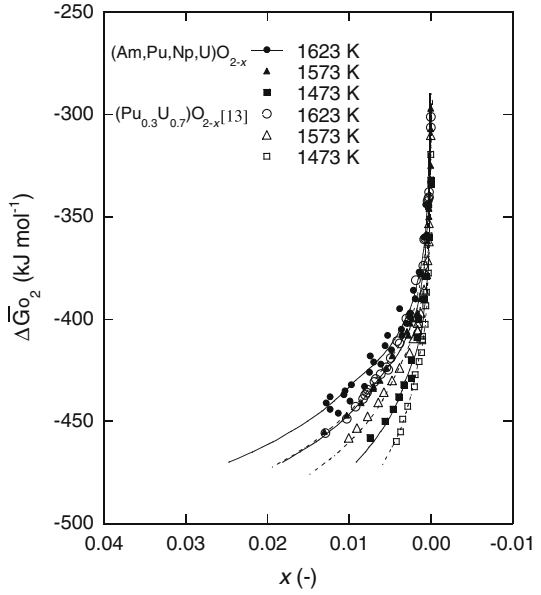

Fig. 5. Oxygen potentials of $(Am_{0.02}Pu_{0.30}Np_{0.02}U_{0.66})O_{2-x}$ at temperatures from 1473 to 1623 K.

3.2. Oxygen potentials of $(Am_{0.02}Pu_{0.30}Np_{0.02}U_{0.66})O_{2-x}$

Fig. 5 shows $\Delta\bar{G}_{O_2}$ of $(Am_{0.02}Pu_{0.30}Np_{0.02}U_{0.66})O_{2-x}$ as a function of O/M at three different temperatures. The literature values of $(Pu_{0.3}U_{0.7})O_{2-x}$ are also shown for comparison. The $\Delta\bar{G}_{O_2}$ of $(Am_{0.02}Pu_{0.30}Np_{0.02}U_{0.66})O_{1.9900}$ is −440 kJ mol^{-1} at 1623 K, and it is 10 kJ mol^{-1} higher than $\Delta\bar{G}_{O_2}$ of $(Pu_{0.3}U_{0.7})O_{1.990}$. The relation between $\ln p^*_{O_2}$ and $1/T$ is shown in Fig. 6. The values of $\Delta\bar{H}_{O_2}$ and $\Delta\bar{S}_{O_2}$ are calculated using Eq. (6) and are listed in Table 1. The $\Delta\bar{H}_{O_2}$ of $(Am_{0.02}Pu_{0.30}Np_{0.02}U_{0.66})O_{2-x}$ are 102–149 kJ mol^{-1} higher than $\Delta\bar{H}_{O_2}$ of $(Pu_{0.3}U_{0.7})O_{2-x}$.

It was suggested by X-ray diffraction analysis that $(Am_{0.02}Pu_{0.30}Np_{0.02}U_{0.66})O_{2-x}$ is a solid solution compound [6], and Bartscher and Sari [27] reported $\Delta\bar{G}_{O_2}$ of NpO_{2-x}, with $\Delta\bar{H}_{O_2}$ and $\Delta\bar{S}_{O_2}$ of $NpO_{1.995}$ as −1144 kJ mol^{-1} and −374 J mol^{-1} K^{-1}, respectively. The values of $\Delta\bar{G}_{O_2}$ for NpO_{2-x} are lower than those for $(Pu_{0.2}U_{0.8})O_{2-x}$. It was well-known that $\Delta\bar{G}_{O_2}$ for AmO_{2-x} is significantly higher than those of the MOX, like that of PuO_2 [28,29]. Osaka et al. [30] reported the effect of Am content on $\Delta\bar{G}_{O_2}$ of MOX; Am addition to MOX increased $\Delta\bar{G}_{O_2}$. The increase of $\Delta\bar{G}_{O_2}$ of $(Am_{0.02}Pu_{0.30}Np_{0.02}U_{0.66})O_{2-x}$ observed in the present study might be due to Am content.

The higher O/M molar ratio was obtained for the MOX including MAs. The differences of O/M ratio between samples with and without MA elements are estimated to be 0.005 and 0.002 at temperatures of 1623 and 1473 K, respectively, under the condition $\Delta\bar{G}_{O_2}$ = −450 kJ mol^{-1} (see Fig. 5). It may be shown that the effect of adding MA to the MOX fuel on FCCI is not significant.

Table 1
$\Delta\bar{H}_{O_2}$ and $\Delta\bar{S}_{O_2}$ in $(Pu_{0.2}U_{0.8})O_{2-x}$, $(Pu_{0.3}U_{0.7})O_{2-x}$ [13] and $(Am_{0.02}Pu_{0.30}Np_{0.02}U_{0.66})O_{2-x}$.

x	$(Pu_{0.2}U_{0.8})O_{2-x}$		$(Pu_{0.3}U_{0.7})O_{2-x}$		$(Am_{0.02}Pu_{0.30}Np_{0.02}U_{0.66})O_{2-x}$	
	ΔS_{O_2} (J mol^{-1} K^{-1})	ΔH_{O_2} (kJ mol^{-1})	ΔS_{O_2} (J mol^{-1} K^{-1})	ΔH_{O_2} (kJ mol^{-1})	ΔS_{O_2} (J mol^{-1} K^{-1})	ΔH_{O_2} (kJ mol^{-1})
0.001	−374	−994	−230	−750	−171	−648
0.003	−383	−1038	−267	−839	−183	−698
0.005	−397	−1083	−300	−922	−223	−773

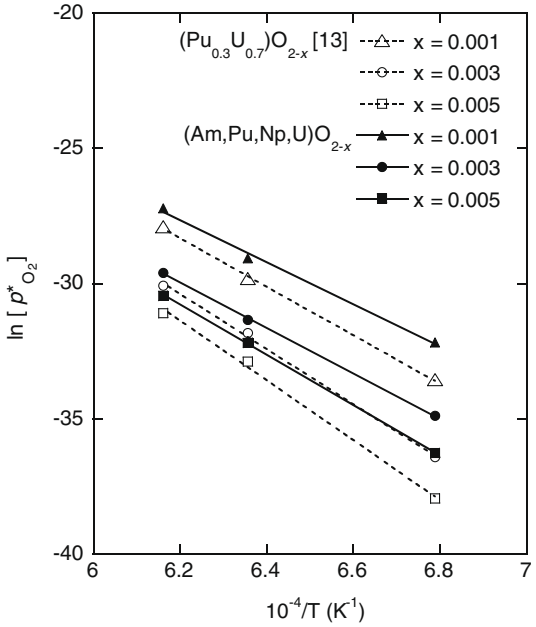

Fig. 6. Relation between $\ln p^*_{O_2}$ and $1/T$ in $(Am_{0.02}Pu_{0.30}Np_{0.02}U_{0.66})O_{2-x}$ and $(Pu_{0.3}U_{0.7})O_{2-x}$.

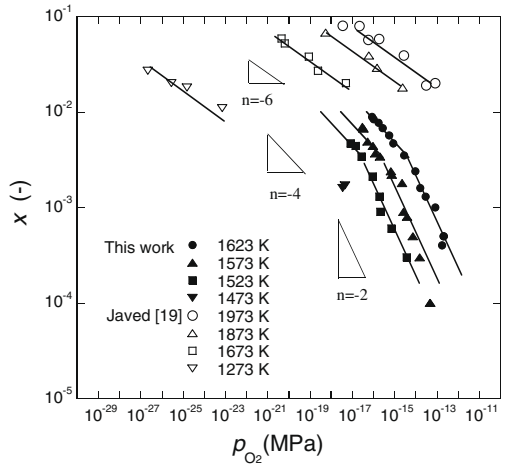

Fig. 7. Plot of oxygen partial pressure versus x in $(Pu_{0.2}U_{0.8})O_{2-x}$.

3.3. Evaluation based on lattice defect theory

Figs. 7 and 8 show the relationships between x in MO_{2-x} and p_{O_2}. The relation can be evaluated by lattice defect theory [31–33] and is generally given by,

$$X \alpha p_{O_2}^{1/n}, \tag{7}$$

where n is a characteristic number identifying the type of lattice defect. For $(Pu_{0.2}U_{0.8})O_{2-x}$, $n = -2$ near the stoichiometric composition, and the value of n changes to -4 with decreasing the O/M molar ratio(see Fig. 7). Previously, it was found that n in the relation for $(Pu_{0.3}U_{0.7})O_{2-x}$ varied from -2 to -3 with increasing x [13]. These variations of n show that the type of defect changes with Pu content. The anion in a fluorite structure has four first neighbor cations. For MOX with less than 20% Pu, the average number of neighbor Pu ions are less than one. For MOX with more than 30% Pu it is more than two. The valence of Pu ions changes from +4 to +3 with decreasing the O/M molar ratio. This means that the number of Pu ions around the oxygen vacancy is the key parameter to determine which type of lattice defect is generated. Fig. 8 shows the dependency of oxygen partial pressure on the deviation x for the MOX of $(Am_{0.02}Pu_{0.30}Np_{0.02}U_{0.66})O_{2.00-x}$. The relationship for the MOX of $(Pu_{0.3}U_{0.7})O_{2-x}$ [13] is also shown in Fig. 8 for comparison. In the hypo-stoichiometric region, the value of n is expressed by -2 near the stoichiometric composition, and it is -3 in the region of low O/M molar ratio.

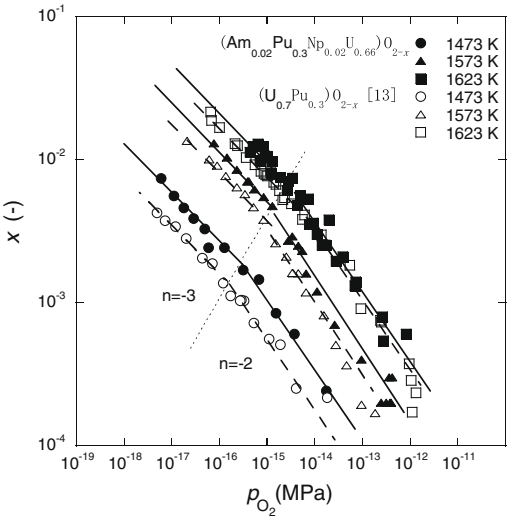

Fig. 8. Plot of oxygen partial pressure versus x in $(Am_{0.02}Pu_{0.30}Np_{0.02}U_{0.66})O_{2-x}$.

4. Conclusion

The $\Delta\bar{G}_{O_2}$ values for $(Pu,U)O_{2-x}$ and $(Am, Pu, Np, U,)O_{2-x}$ have been measured as a function of O/M molar ratio and temperature. The following may be concluded.

(1) The $\Delta\bar{G}_{O_2}$ of $(Pu_{0.2}U_{0.8})O_{2-x}$ were about 25 kJ mol^{-1} lower than those of $(Pu_{0.3}U_{0.7})O_{2-x}$. The current data were consistent with calculated values derived from the model of Besmann and Lindemer and represented well the effect of the Pu function on the $\Delta\bar{G}_{O_2}$.

(2) The $\Delta\bar{G}_{O_2}$ of $(Am_{0.02}Pu_{0.30}Np_{0.02}U_{0.66})O_{2-x}$ were slightly higher than those of $(Pu_{0.3}U_{0.7})O_{2-x}$. The difference of $\Delta\bar{G}_{O_2}$ between the two oxides is very small, it may be concluded that the effect of MA addition to MOX fuel on the FCCI is not significant.

(3) The relationship between p_{O_2} and x in MO_{2-x} was analyzed based on lattice defect theory. The relationships $x \alpha p_{O_2}^{-1/2}$ and $x \alpha p_{O_2}^{-1/4}$ were found for $(Pu_{0.2}U_{0.8})O_{2-x}$ depending on x. The relationships between p_{O_2} and x in $(Am_{0.02}Pu_{0.30}Np_{0.02}U_{0.66})O_{2-x}$ varied from $x \alpha p_{O_2}^{-1/2}$ to $x \alpha p_{O_2}^{-1/3}$ with O/M molar ratio, which were the same as obseved for $(Pu_{0.3}U_{0.7})O_{2-x}$.

Acknowledgements

The authors are pleased to acknowledge Mr H. Uno and Mr T. Sunaoshi for their collaboration in the sample preparation. Special thanks are due to Dr S. Nagai and Dr Nakae for valuable discussions.

References

[1] M. Katsuragawa, H. Kashihara, M. Akebi, J. Nucl. Mater. 204 (1993) 14.
[2] S. Nomura, A. Aoshima, T. Koyama, M. Myochin, in: Proceedings of Global 2001, 9–13 September, Paris, France, 2001, p. 42.
[3] Y. Sagayama, in: Proceedings of Global 2005, 9–13 October, AESJ, Tsukuba, Japan, 2005, p. 380.

[4] T. Iwamura, Trans. Am. Nucl. Soc. 96 (2007) 743.
[5] K. Morimoto, M. Ogasawara, H. Uno, M. Kato, Y. Kihara, in: Proceedings of Global 2005, 9–13 October, AESJ, Tsukuba, Japan, 2005, p. 137.
[6] M. Kato, H. Uno, T. Tamura, K. Morimoto, K. Konashi, Y. Kihara, Rec. Adv. Actin. Sci. (2006) 367.
[7] T.L. Markin, R.S. Street, J. Inorg. Nucl. Chem. 29 (1967) 2265.
[8] C. Sari, U. Benedict, H. Blank, J. Nucl. Mater. 35 (1970) 267.
[9] M. Kato, K. Morimoto, H. Sugata, K. Konashi, M. Kashimura, T. Abe, Trans. Am. Nucl. Soc. 96 (2007) 193.
[10] K. Morimoto, M. Kato, M. Ogasawara, M. Kashimura, J. Nucl. Mater. 374 (2008) 378.
[11] J.J. Carbajo, G.L. Yoder, S.G. Popov, V.K. Ivanov, J. Nucl. Mater. 299 (2001) 181.
[12] M. Kato, S. Nakamichi, T. Takano, in: Proceedings of Global 2007, 9–13 September, ANS, Boise, Idaho, US, 2007, p. 916.
[13] M. Kato, T. Tamura, K. Konashi, S. Aono, J. Nucl. Mater. 344 (2005) 235.
[14] T.L. Markin, E.J. McIver, in: Plutonium 1965, Barnes and Noble, New York, 1967, p. 845.
[15] The Plutonium–Oxygen and Uranium–Plutonium-Oxygen Systems: A Thermochemical Assessment, Tech. Repot Ser. No.79, IAEA, Vienna, 1967, p. 52.
[16] G.R. Chilton, J. Edwards, United Kingdom Atomic Energy Authority Northern Division Report, ND-R-276(W), 1980.
[17] J. Edwards, R.N. Wood, G.R. Chilton, J. Nucl. Mater. 130 (1985) 505.
[18] G.R. Chilton, I.A. Kirkham, in: Plutonium and Other Actinides, Elsevier, New York, 1976, p. 171.
[19] N.A. Javed, J. Nucl. Mater. 47 (1973) 336.
[20] R.E. Woodley, J. Nucl. Mater. 96 (1981) 5.
[21] R.E. Woodley, M.G. Adamson, J. Nucl. Mater. 82 (1985) 65.
[22] M. Tetenbaum, IAEA-SM-190/41 (1975) 305.
[23] O.T. Sørensen, in: Plutonium and Other Actinides, Elsevier, New York, 1976, p. 123.
[24] P.E. Blackburn, J. Nucl. Mater. 46 (1973) 244.
[25] P.E. Blackburn, C.E. Johnson, IAEA-SM-190/50 (1974) 17.
[26] T.M. Besmann, T.B. Lindemer, J. Nucl. Mater. 130 (1985) 489.
[27] W. Bartscher, C. Sari, J. Nucl. Mater. 140 (1986) 91.
[28] C. Thiriet, R.J.M. Konings, J. Nucl. Mater. 320 (2003) 292.
[29] T.D. Chikalla, L. Eyring, J. Inorg. Nucl. Chem. 29 (1967) 2281.
[30] M. Osaka, K. Kurosaki, S. Yamanaka, J. Alloys Comp. 428 (2007) 355.
[31] G. Brouwer, Philips Res. Rep. 9 (1954) 366.
[32] P. Kofstad, Nonstoichiometry, Diffusion, and Electrical Conductivity in Binary Metal Oxides, John Wiley, New York, 1972.
[33] O.T. Sørensen, Nonstoichimetric Oxides, Academic Press, New York, 1981. p. 1.